

UKAEA RESEARCH GROUP

Preprint

SELECTIVE MULTI-PHOTON DISSOCIATION
OF SULPHUR HEXAFLUORIDE

H N RUTT

CULHAM LABORATORY
Abingdon Oxfordshire

1977

This document is intended for publication in a journal or at a conference and is made available on the understanding that extracts or references will not be published prior to publication of the original, without the consent of the authors.

Enquiries about copyright and reproduction should be addressed to the Librarian, UKAEA, Culham Laboratory, Abingdon, Oxfordshire, England

SELECTIVE MULTI-PHOTON DISSOCIATION
OF SULPHUR HEXAFLUORIDE

H.N. Rutt

UKAEA Culham Laboratory, Abingdon, OX14 3DB, UK.

ABSTRACT

Isotopically-selective multi-photon dissociation of SF₆ by CO₂ laser irradiation has been measured in a focused geometry. The variation of dissociation with laser energy and wavelength has been investigated in detail and strong enrichment of S³⁴ was obtained. A threshold intensity of $\lesssim 60 \text{ MW/cm}^2$ was observed, despite the use of H₂ scavenger gas. Under the conditions of the experiment an upper limit of $\lesssim 0.2 \text{ cm}^{-1}$ was established for spectral broadening of transmitted radiation, and of $\leq 10^{-6}$ for the intensity of any scattered side-band radiation within 10 cm^{-1} of the exciting line.

(Submitted for publication in Journal of Physics D)

September 1976.

1. INTRODUCTION

Considerable interest has been shown in the recently discovered isotopically selective collisionless multi-photon dissociation of polyatomic molecules by intense infra-red laser radiation, (Ambartsumyan et al, 1976a). This paper discusses our initial work on this process; during the course of the experiments a number of other papers have appeared (Hancock, 1976; Lyman and Rockwood, 1976; Ambartsumyan et al, 1976b) which provide additional insight into the physical processes involved. (It is perhaps interesting to note that the theory of multiple quantum transitions was examined as early as 1932, when Majorana calculated the transition probability for magnetic dipole transitions between a group of equi-spaced levels in atoms exhibiting Zeeman splitting of the hyperfine levels. Such transitions were routinely observed in atomic-beam magnetic resonance experiments, e.g. Spalding 1963. The theory was extended to unequally spaced levels by Hack, 1956, and to multi-frequency transitions by Brossel et al, 1955.)

2. EXPERIMENTAL APPARATUS

The CO₂ laser used for these experiments was a Lumonics Model 203, which generated a 10.6 μm pulse of 8.5J at a repetition rate of 1 Hz. The laser was modified at Culham to give a peak-to-peak stability of $\pm 5\%$. SF₆ gas was irradiated in a stainless steel cell of 38 mm internal diameter and 100 mm length, having two vacuum connections. A 53 mm focal length anti-reflection coated germanium lens was used as the input window to the cell, and the output window was an anti-reflection coated germanium flat. Three windows of germanium, silica or potassium bromide were additionally provided around the focal region, for observation of side-light. The cell was pumped to $\sim 10^{-5}$ torr, and was gently

baked (to $\sim 100^{\circ}\text{C}$). (Higher temperature baking is precluded by the infra-red windows.) The vacuum system permits the examination of a sample of irradiated gas by trapping in a small liquid nitrogen cooled sidearm, which may subsequently be valved off and removed. This arrangement permits several experiments to be run sequentially, with the samples analysed later. It is also possible to flow gas through the cell when necessary.

5. EXPERIMENTAL PROCEDURE

Early experiments showed that whilst multi-photon dissociation of SF_6 is readily demonstrated, the results can exhibit lack of reproducibility unless all conditions are carefully controlled - in particular the output of the laser. The following precautions also reduced the scatter in the results:

- (a) The gas mixture in the laser was carefully standardized since different gas mixes produced different pulse shapes (having similar total energies);
- (b) To avoid variation in the gas mix used for the multi-photon experiments a pre-mixed cylinder containing 10% SF_6 in hydrogen was used;
- (c) All-metal pipework was used to connect the cylinder to the experiment. (Slow loss of hydrogen by diffusion through plastic tubing leads to a steady increase in the SF_6 concentration.)
- (d) After any exposure to air the cell was pumped to $\sim 10^{-5}$ torr and gently baked. It was then conditioned by exposure to 1 torr of the SF_6/H_2 gas mix for 24 hours;
- (e) To obtain maximum reproducibility the laser was not turned off between experiments, but rather the beam was dumped.
- (f) The samples were condensed into the removable side arm for a fixed length of time (5 minutes). At 77°K the vapour pressure of SF_6 is only $\approx 7.5 \times 10^{-7}$ torr, so that at the partial pressures of SF_6 typically used (0.1 torr) essentially all the SF_6 should be condensed into the trap. In practice

this took some time, owing to the restricted vacuum conductance from the cell to the trap. After 5 minutes > 99% of the SF₆ had been trapped. This time is counted from the point at which the trap cools to 77°K, since the vapour pressure is a very rapid function of temperature (e.g. 0.5 torr at 120°K).

- (g) The sample pressure was set with a McLeod gauge. This avoided calibration difficulties with electrical gauges, and also avoided any possibility of slow reaction in the mixture caused by the hot filament of a Pirani gauge.

Except when otherwise stated, all experiments were performed with 360 shots at 1 torr total pressure in the focused geometry already described.

4. SAMPLE ANALYSIS

Samples were analysed for isotopic composition by infra-red absorption measurements. The lines from S³⁴F₆ and S³²F₆ overlap slightly due to hot-band structure, and the effect of this overlap was removed by calibration with control samples of natural isotopic abundance. The S³³F₆ peak is not resolvable at room temperature. In order to obtain consistent results the sample gas cell was allowed to reach thermal equilibrium in the spectrophotometer, since the hot band structure changes slightly during the rise of a few degrees caused by the infra-red beam. With careful handling, absorption values were reproducible to better than ± 1% absolute and this determined the error limits on measurements of dissociation.

Mass spectrometer analysis was also attempted on an Edwards 60° sector mass spectrometer with a simple capillary inlet system. Results from this instrument were less reproducible and it is probable that a more sophisticated inlet system is needed. (A further problem was that the limited resolution available enforced the use of the m/e = 89 peak which corresponds to an SF₃⁺ fragment. Since this is the principal peak observed in the SF₄ mass spectrum, confusion can arise unless full spectra are taken and fitted. The possible presence of unusual compounds which could give SF₃⁺ fragments of the same mass cannot be neglected.) For these reasons infra-red measurements were used exclusively for the

results given here, since they are considered to be more reliable. Typical infra-red spectra are shown in Fig.1.

No evidence for back-reactions was seen when the post irradiation SF_6 content was measured continuously over a period of 8 hours.

5. ISOTOPE ENRICHMENT RESULTS

5.1 Enrichment as a Function of the Number of Laser Pulses

Fig.2 shows an exponential dependence on the number of shots, although there are indications that the first few tens of shots cause excess dissociation. (Note that the naturally-occurring ratio of C^{34}/C^{32} is 4.22%.) The exponential dependence leads to a convenient definition of the extent of dissociation (D):

$$D^{32} = 1 - [C^{32}/C^{32} \text{ initial}]^{1/M} \quad \dots (1)$$

where M is the number of shots and C^{32} the concentration of $S^{32}F_6$.

5.2 Dissociation as a Function of Laser Pulse Energy

The laser energy delivered to the cell was varied by means of calibrated polythene attenuators. In this way the time history of the laser remained unaffected, although the focal spot may be enlarged by the poor optical quality of the polythene. The results are plotted in Fig.3 on a log-log scale, and show that D^{32} varies approximately as $E^{3/2}$, as noted recently by Cotter and Fuss (1976).

5.3 Dissociation as a Function of Laser Wavelength

Fig.4 shows the variation in the degree of dissociation as the laser is tuned from the line P(10) to P(36), together with the variation in the laser energy output. For the relatively low gain lines below P(10) and above P(28) the beam pattern becomes less uniform, and more critically dependent on alignment. In Fig.5 the data are replotted by removing the laser energy dependence, assuming that the $E^{3/2}$ dependence demonstrated for the P(20) is also valid for other lines. The positions of peak linear adsorption in $S^{32}F_6$ and $S^{34}F_6$ are marked for reference.

For R(14), R(22) and R(30) of the 10.6 μm band with 5.5, 7 and 4.5J respectively, no dissociation was detected at a level of $< 8 \times 10^{-5}$ per shot.

5.4 Additional Experiments on the Intensity Dependence

Using an unfocused beam approximately 5 cm^2 in area of 8.5J in P(20) the cell was irradiated for 3600 shots. Although a very slight drop occurred in the concentration of $\text{S } ^{32}\text{F}_6$, it was within the limits of experimental error. Under these conditions the dissociation rate is $\leq 8 \times 10^{-6}$ per pulse. Using a weakly focused beam of $\sim 0.7 \text{ cm}^2$ area for 360 shots the limit is $\leq 8 \times 10^{-5}$ per pulse. Under these conditions the intensities averaged over the 100 ns gain-switched spike of the laser (which contains $\sim \frac{1}{2}$ of the total energy) are $\sim 8.5 \text{ MW/cm}^2$ and $\sim 60 \text{ MW/cm}^2$ respectively; the KBr cell windows fail at $\leq 100 \text{ MW/cm}^2$.

6. SPECTROSCOPIC EXPERIMENTS

6.1 Visible Region

No visible/near UV emission could be reliably detected during the multi-photon experiments. The emission of such radiation does appear to depend on some as yet uncharacterised experimental parameter, since in very early experiments green emission from the focal volume was seen. This emission has not recurred.

6.2 Infra-red Emission

Searches have been made for line broadening of the transmitted laser light, and for scattered sidebands. With a resolution of $\sim 0.2 \text{ cm}^{-1}$ FWHM no broadening of the transmitted light was detected. Observation of the focal volume at right angles to the direction of beam propagation showed no scattered light in a region $\pm 10 \text{ cm}^{-1}$ from the P(20) line. Taking into account the geometrical factors and noise level, the detection limit was $\leq 10^{-6}$ of the incident radiation scattered isotropically into 1 cm^{-1} .

This limit assumes correct alignment; improvements are in hand to provide a more precise alignment procedure. These measurements were made with the SF_6/H_2 mixture flowing, to avoid depletion of the SF_6 .

7. DISCUSSION

7.1 Variation with the Number of Laser Pulses

The dependence of the degree of dissociation on the number of shots is exponential with

the exception of the first few tens of shots. An exponential dependence implies a constant fraction dissociated per shot, as expected for a uni-molecular process. The slight excess dissociation caused by the first few shots could be caused by heating of the gas reducing dissociation in later shots, since the effect disappears when the cell has time to reach thermal equilibrium.

7.2 Dissociation as a Function of Pulse Energy

Let us postulate that the proportion of the volume irradiated which dissociates may be represented by

$$Q = 1 \quad I \geq I_S \quad \dots (2)$$

$$Q = \left[\frac{I}{I_S}\right]^N \quad I \leq I_S \quad \dots (3)$$

where I is the intensity incident on the volume. For a total incident power P contained in a circular beam of radius r and focused by a lens of focal length F acting as the window of a cell of length $2F$, the volume V is then given by

$$\frac{V}{2} = \pi a^2 \int_0^R x^2 dx + \pi a^2 \int_R^F x^2 \left[\frac{P}{\pi a^2 x^2 I_S} \right]^N dx \quad \dots (4)$$

where x is a position variable with $x = 0$ at the focus, and

$$R = \frac{1}{a} \left[\frac{P}{I_S \pi} \right]^{\frac{1}{2}} \quad \dots (5)$$

$$a = r/F \quad \dots (6)$$

Geometric optics are assumed, and laser beam depletion is neglected. The small-signal absorption was 35% at the peak of the $S^{32}F_6$ band; however the measured absorption under high intensities was always $< 10\%$, justifying the neglect of laser beam depletion.

Hence

$$\frac{V}{2} = \frac{1}{3\pi^{\frac{1}{2}} a} \left[\frac{P}{I_S} \right]^{3/2} + \left[\frac{P}{I_S} \right]^N \left[\frac{1}{\pi a^2} \right]^{N-1} \frac{1}{3-2N} \left\{ F^{3-2N} - \left[\frac{P}{I_S \pi} \right]^{\frac{3-2N}{2}} a^{2N-3} \right\} \dots (7)$$

$$N \neq 1.5$$

The measured (mean) dissociation per shot plotted in Figs.1-4 is simply

$$D = V/\text{total volume} \quad \dots (8)$$

The parameters relevant to the results plotted in Fig.3 are

$$F = 5\text{cm} \quad r = 1.5\text{ cm} \quad P \approx 40\text{ MW (gain switched spike only)}$$

In Fig.3 the predictions of eqn.7 are plotted for various values of I_S and N . Values of I_S and N have been chosen which fit the absolute value of dissociation for the maximum power available ~ 40 MW. The best fit to the data is given by $I_S = 125\text{ MW/cm}^2$ and $N = 3.2$, although the curve for $I_S = 250\text{ MW/cm}^2$ and $N = 1.65$ also falls within the error bars. The measured results are thus relatively insensitive to the exact values of N and I_S . The two lowest energy points in Fig.3 fall well below the $E^{3/2}$ line, which is the steepest slope which eqn.7 can assume as $N \rightarrow \infty$. Thus the dissociation falls off more rapidly at low intensities, a result which is also supported by the additional measurements with unfocused beams.

Table 1 summarises the value of D predicted for various N , I_S pairs in the appropriate geometry. In all cases dissociation should have been seen if the $(I/I_S)^N$ power law was followed as $I \rightarrow 0$. There is thus strong evidence of a 'threshold' behaviour in the intensity dependence, or at least a rapid steepening of the slope for $I \lesssim 60\text{ MW/cm}^2$. The absolute powers quoted depend on the observation that ~ 0.4 of the laser energy is contained in the first 80 ns gain switched spike, and the assumption that only this spike is relevant to dissociation. Sub-structure in the spike is ignored. Modifications to these values will simply scale I_S and P appropriately without changing the conclusions.

7.3 Dissociation as a Function of Wavelength

Interpretation of these results is complicated by variations in laser energy output and beam intensity distribution as the laser is tuned. Within the range P(26) to P(12) these variations are less than $\pm 6\%$, but for the lower gain lines the beam pattern becomes severely striated, leading to variations in the geometrical factors which affect the dissociation rate (eqn.7).

In Fig.5 the line variation with laser wavelength is replotted, by assuming that the $E^{3/2}$ variation measured for P(20) is valid for all lines. The effect of striations was especially noticeable for the line P(30), and this is almost certainly the reason for this point lying well

above the other results.

However, within the range P(26) to P(12) the renormalization should be valid, since the beam intensity distribution remains reasonably constant. In this range the dissociation curve is seen to be fairly flat on the low frequency side of the $S^{32}F_6$ fundamental, and falls sharply on the high frequency side. It is clearly wider than the linear absorption curve (Fig.1). This is consistent with pumping on the low frequency side helping to cancel out anharmonicity. The skewed shape of the renormalized curve of Fig.5 implies that selective dissociation of $S^{34}F_6$, leaving $S^{32}F_6$ unaffected, would be more difficult to achieve. The dissociation observed in the regions P(26) to P(34) and for the line P(10) does not, on first consideration, appear consistent with the high isotopic enrichments which have been achieved. However, the unexpectedly high dissociation rates observed at CO_2 wavelengths so far removed from the $S^{32}F_6$ absorption band is due to the tendency of the TEA laser to become more strongly striated on these low gain lines, thus increasing the geometrical factors in eqn.7 and invalidating the renormalization used in the P(26)-P(34) and P(10) regions of Fig.5.

Thus, these experiments show that definitive results on the variation of D with wavelength clearly require very careful control of the intensity distribution.

8. CONCLUSIONS

The (skewed) wavelength dependence of the multi-photon dissociation process in SF_6 has been measured in a focused geometry, under conditions in which a high S^{32}/S^{34} isotopic selectivity has been achieved.

The dependence of the measured dissociation rate on the assumed form of the variation of this rate with laser energy has been examined in some detail. The results support the existence of a 'threshold' at low intensity values, as reported by Ambartsumyan et al, 1976c, and suggest the experimental importance of spatial mode control on low gain CO_2 transitions. It should be noted that a 'threshold' is seen, despite the use of a scavenger gas (H_2). Some controversy has existed over the existence of such a threshold, and in previous work the absence of a threshold behaviour has been correlated with the use of a scavenger (Ambartsumyan, 1976).

ACKNOWLEDGEMENTS

The author wishes to thank Dr. A.C. Walker for his help in the initial phases of these experiments.

REFERENCES

- AMBARTSUMYAN, R.V., GOROKHOV, Y.A., LETOKHOV, G.N., MAKAROV, R.A., RYABOV, E.A., CHEKALIN, N.V. - Sov.J.QE 5, No.10, pp.1196-1198, 1975
- AMBARTSUMYAN, R.V., GOROKHOV, Y.A., LETOKHOV, V.S., PURETSKII, A.A. - JEPT Lett. 22, No.7, pp.177-178, 5 Oct.1975
- AMBARTSUMYAN, R.V., GOROKHOV, Y.A., LETOKHOV, V.S., MAKAROV, R.A., PURETSKII, A.A., FURZIKOV, N.P. - JETP Lett. 23, No.4, pp.217-220, Feb.1976
- AMBARTSUMYAN, R.V. - Tunable lasers and Applications Conference, Loen, Norway, June 1976
- BROSSEL, MARGERIE AND WINTER - Compt.Rendue, Acad.Sci.Paris, 241, 556 and pp.600, 1955
- COTTER, T.P., FUSS, W. - Optics Communications 18, 31, 1976
- HANCOCK, G., CAMPBELL, J.O., WELGE, K.H. - Optics Communications 16, No.1, pp.177-181, Jan.1976
- HACK, M.N. - Phys.Rev. 104, 84, 1956
- LYMAN, J., JENSEN, R.J., RINK, J., ROBINSON, C.P., ROCKWOOD, S.D. - LASL Report No. UR-75-707, 1976
- LYMAN, J.L., ROCKWOOD, S.D. - J.Appl.Phys. 47, No.2, pp.595-601, Feb.1976
- MAJORANA, E. - Nuovo Cimento 9, 43, 1932
- SPALDING, I.J. - Proc.Phys.Soc. 81, 156, 1963

TABLE 1

N	I _s	D for I = 8MW/cm ² Z = 0.44	D for I = 57MW/cm ² Z = 0.062
0.91	1250	4.40 x 10 ⁻³	3.70 x 10 ⁻³
0.97	1000	4.06 x 10 ⁻³	3.85 x 10 ⁻³
1.05	750	3.74 x 10 ⁻³	4.14 x 10 ⁻³
1.20	500	3.08 x 10 ⁻³	4.58 x 10 ⁻³
1.65	250	1.50 x 10 ⁻³	5.41 x 10 ⁻³
3.20	125	6.60 x 10 ⁻⁵	5.02 x 10 ⁻³
Detection limit		8 x 10 ⁻⁶	8 x 10 ⁻⁵

Z = fraction of total cell volume irradiated

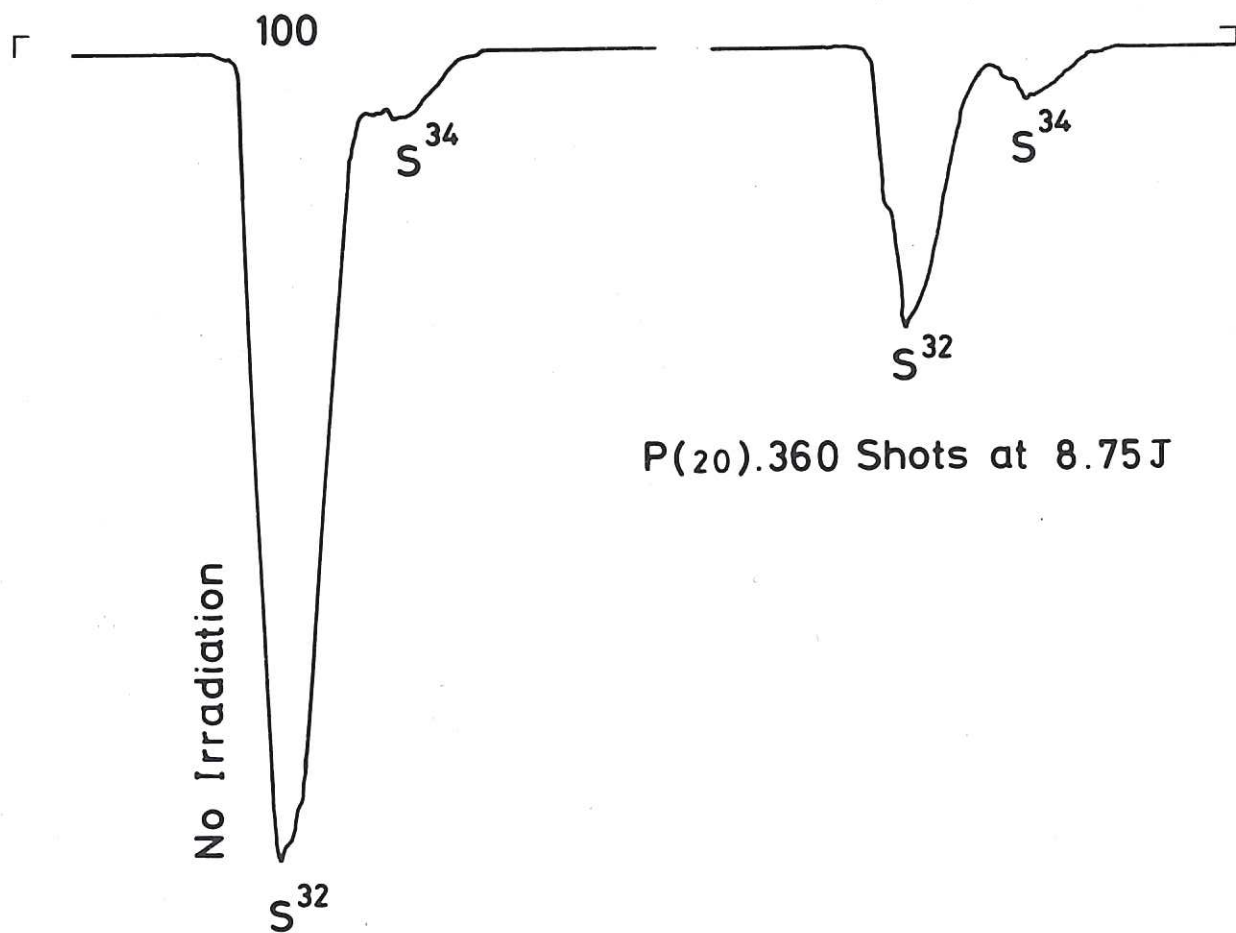


Fig.1 SF₆ IR absorption spectra, before and after irradiation by 360 pulses of 8.75J at CO₂P(20).

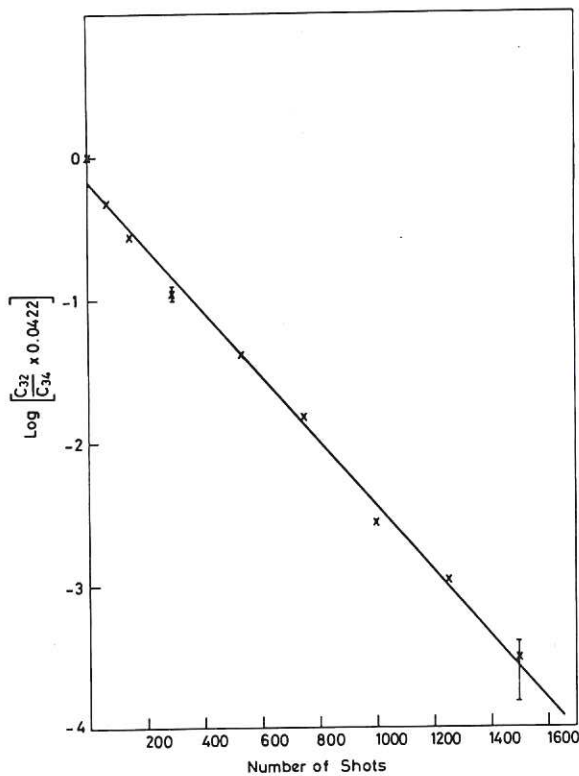


Fig.2 Enrichment as a function of number of shots.

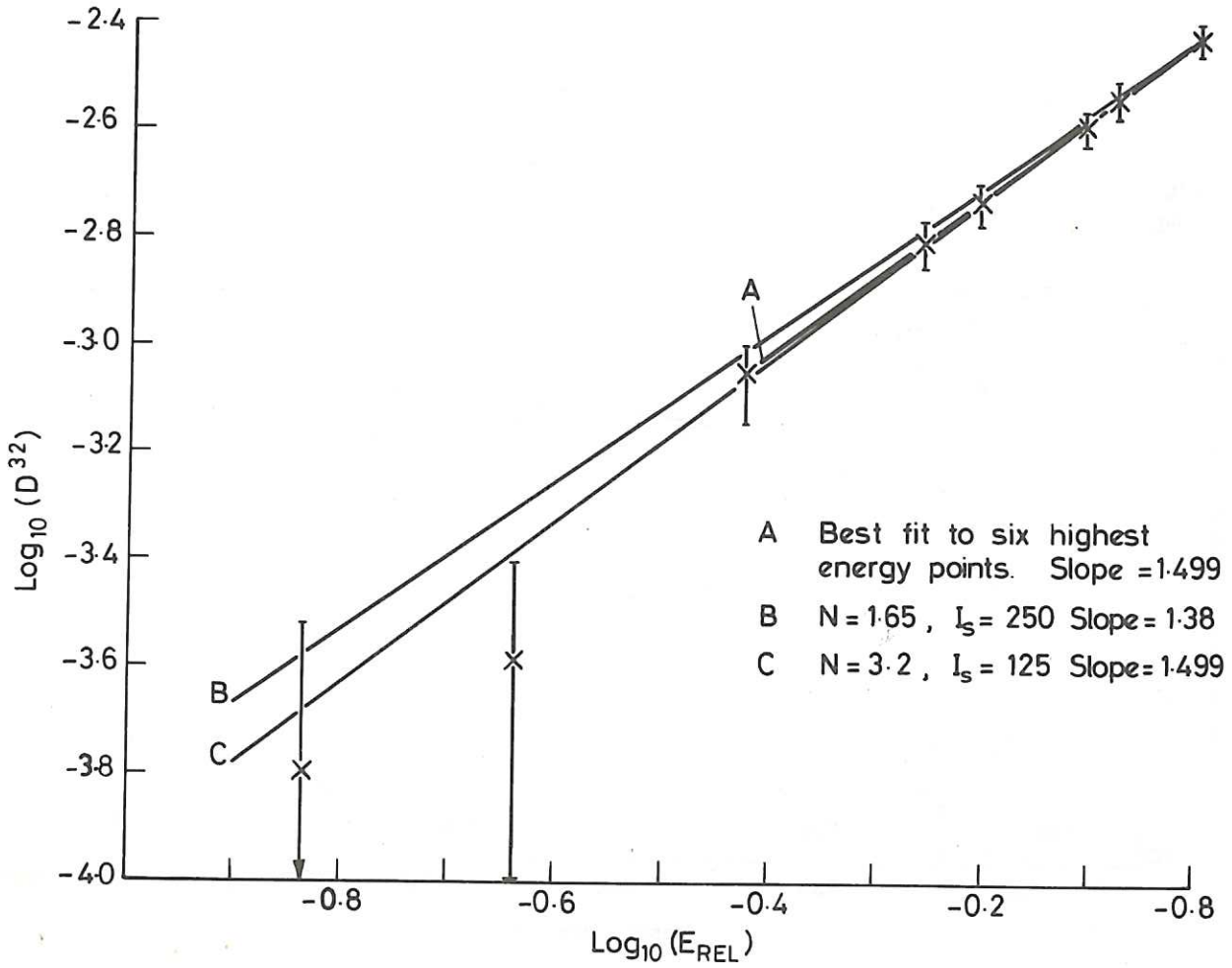


Fig.3 Dissociation as a function of energy per pulse, using P(20) irradiation.

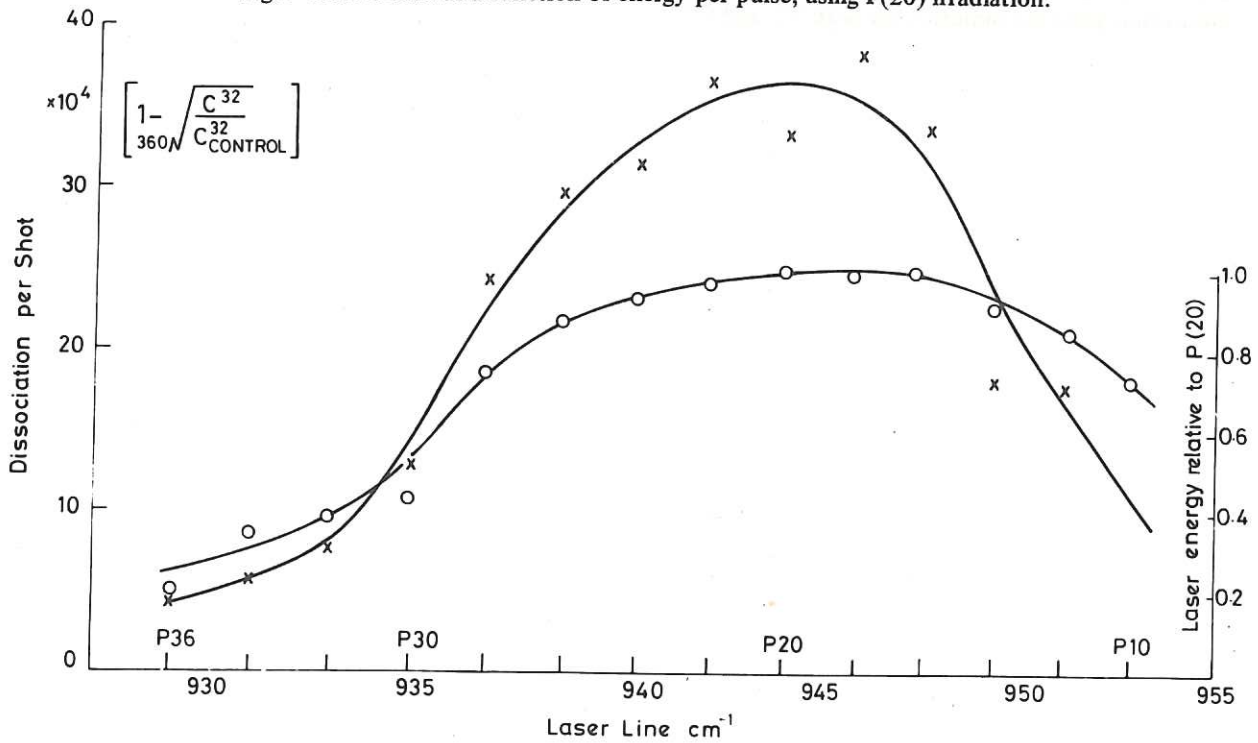


Fig.4 Dependence of dissociation (X) on laser wavenumber, (data not corrected for laser energy variation, shown circled).

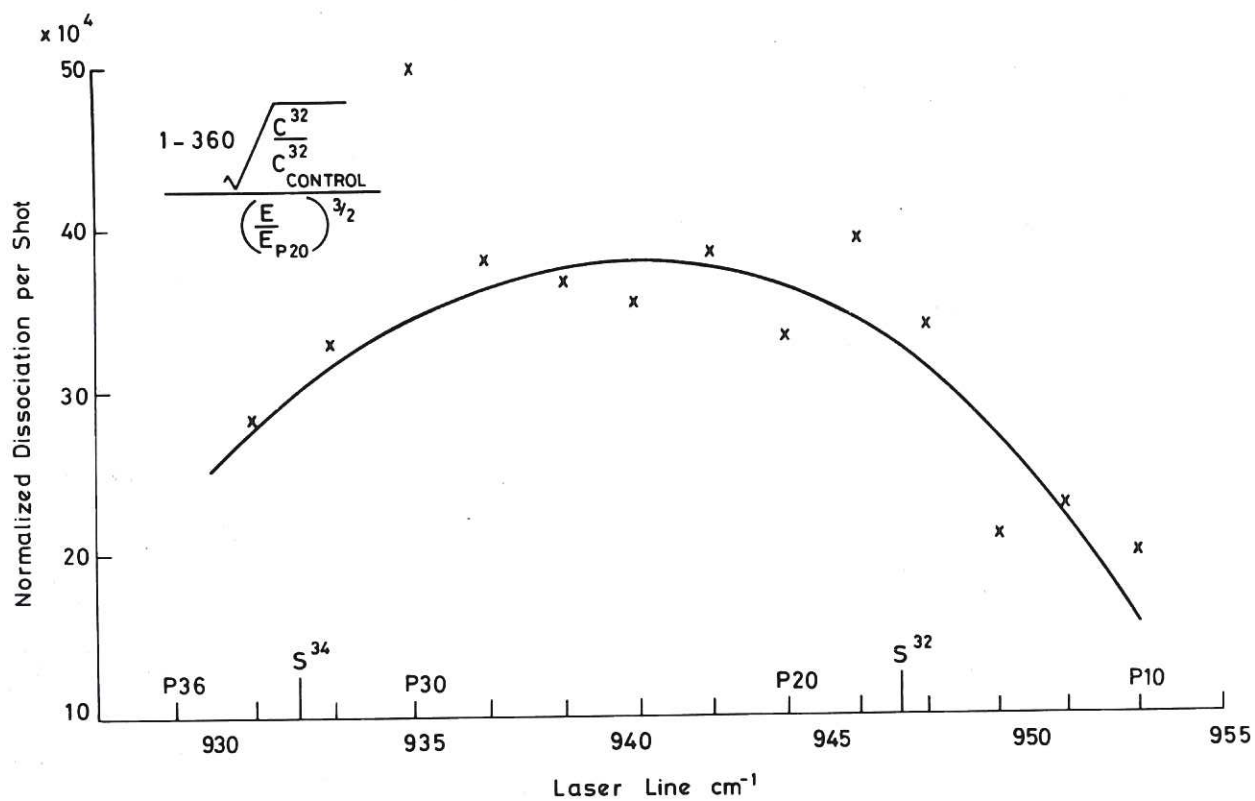


Fig.5 Dependence of dissociation on laser wavenumber, corrected for laser energy variation. (Low-intensity SF₆ absorption peaks are indicated for both S³² and S³⁴.)

The first part of the document discusses the importance of maintaining accurate records of all transactions. It emphasizes that every entry, no matter how small, should be recorded to ensure the integrity of the financial statements. This includes not only sales and purchases but also expenses, income, and any other financial activity. The document also highlights the need for regular reconciliation of accounts to identify any discrepancies early on.

Next, the document covers the various methods used to record transactions. It explains the difference between single-entry and double-entry bookkeeping systems. Double-entry bookkeeping is preferred because it provides a more comprehensive view of the company's financial position by recording each transaction in two accounts: a debit and a credit. This system helps in detecting errors and ensures that the accounting equation remains balanced.

The document then discusses the importance of using standardized accounting principles and practices. This includes following generally accepted accounting principles (GAAP) to ensure that the financial statements are comparable and reliable. It also mentions the need for proper documentation and supporting evidence for all transactions, such as invoices, receipts, and contracts.

Finally, the document concludes by emphasizing the role of the accounting department in providing accurate and timely financial information to management and other stakeholders. It stresses that good accounting practices are essential for the success and growth of any business.

The first part of the document discusses the importance of maintaining accurate records of all transactions. It emphasizes that every entry, no matter how small, should be recorded to ensure the integrity of the financial data. This includes not only sales and purchases but also expenses and income. The document provides a detailed breakdown of the accounting process, starting from the initial recording of transactions to the final preparation of financial statements. It highlights the need for consistency and accuracy throughout the entire process.

The second part of the document focuses on the classification of transactions. It explains how different types of transactions are categorized into various accounts, such as assets, liabilities, and equity. This classification is essential for understanding the financial position of the business at any given time. The document provides examples of how different transactions are recorded and classified, illustrating the impact of each entry on the financial statements.

The third part of the document discusses the importance of reconciling accounts. It explains how discrepancies between the company's records and the bank's records can be identified and resolved. This process is crucial for ensuring that the company's financial records are accurate and up-to-date. The document provides a step-by-step guide to the reconciliation process, including how to identify errors and how to correct them.

The fourth part of the document focuses on the preparation of financial statements. It explains how the data from the accounting records is used to prepare the balance sheet, income statement, and cash flow statement. The document provides a detailed explanation of each statement and how they are related to each other. It also provides examples of how to prepare each statement, showing the flow of data from the accounting records to the final financial statements.

The fifth part of the document discusses the importance of internal controls. It explains how a system of internal controls can be implemented to prevent and detect errors and fraud. This system includes procedures for authorizing transactions, separating duties, and maintaining accurate records. The document provides a detailed explanation of how to design and implement an effective system of internal controls.

The sixth part of the document focuses on the use of technology in accounting. It explains how accounting software can be used to automate many of the accounting processes, such as recording transactions, reconciling accounts, and preparing financial statements. The document provides a detailed explanation of how to choose and use accounting software, highlighting the benefits of automation and the importance of data security.

The seventh part of the document discusses the importance of ethical considerations in accounting. It explains how accountants must adhere to a code of ethics and maintain the highest standards of integrity and honesty. The document provides a detailed explanation of the ethical principles that guide accountants and how they are applied in practice.

The eighth part of the document focuses on the future of accounting. It discusses the impact of new technologies, such as artificial intelligence and blockchain, on the accounting profession. It also discusses the changing needs of businesses and how accountants must adapt to these changes to remain relevant and effective.